Neuropsychopharmacology (2003) 28, 2010–2019
© 2003 Nature Publishing Group All rights reserved 0893-133X/03 $25.00
www.neuropsychopharmacology.org

In vivo Measurement of the Serotonin Transporter with (*S*)-([^{18}F]fluoromethyl)-(+)-McN5652

P Brust*[,1], R Hinz[2], H Kuwabara[3], S Hesse[4], J Zessin[2], B Pawelke[2], H Stephan[2], R Bergmann[2], J Steinbach[1] and O Sabri[4]

[1]Institute of Interdisciplinary Isotope Research, Leipzig, Germany; [2]Research Center Rossendorf, Institute of Bioinorganic and Radiopharmaceutic Chemistry, Dresden, Germany; [3]Department of Radiology, University of Pittsburgh School of Medicine, Pittsburgh, PA, USA; [4]Clinic for Nuclear Medicine, University of Leipzig, Leipzig, Germany

The radiolabeled serotonin transporter (SERT) ligand [^{11}C](+)-McN5652 has recently been used in clinical positron emission tomography (PET) studies for SERT imaging. However, this radioligand offers disadvantages in routine clinical settings because of its short radioisotope half-life (eg PET facilities within hospitals without a cyclotron need to acquire such radioligands from distant cyclotron units for clinical use). *S*-([^{18}F]fluoromethyl)-(+)-McN5652 ([^{18}F](+)-FMe-McN5652) is an analogue which has been synthesized newly, and has a significantly longer radioisotope half-life. In the porcine brain, it demonstrates the same characteristic distribution pattern of serotonin-uptake sites like the ^{11}C-labeled congener with the highest binding in the midbrain and thalamus and the lowest in the cerebellum and occipital cortex. It shows a 30% higher blood–brain transfer and a slower peripheral metabolism than [^{11}C](+)-McN5652. Rather uniform brain binding was observed after injection of the pharmacologically inactive radiolabeled enantiomer, or after pretreatment with the highly selective SERT inhibitor citalopram. The norepinephrine uptake inhibitor maprotiline did not show any inhibitory effect. Using a one-tissue compartment model (K_1, k''_2) or a two-tissue compartment model (K_1 to k_4) with or without constraints for calculation, the regional binding parameters of [^{11}C](+)-McN5652 and [^{18}F](+)-FMe-McN5652 are highly correlated among each other and with the SERT density, as determined by *in vitro* binding of [^{3}H]citalopram. Using constraints to correct for the free fraction and nonspecific binding of the radiotracers, a considerable increase of the midbrain–occipital cortex ratios with higher values for [^{18}F](+)-FMe-McN5652 compared to [^{11}C](+)McN5652 was revealed. It is concluded that [^{18}F](+)-FMe-McN5652 has better features than [^{11}C](+)McN5652 for SERT imaging with PET.
Neuropsychopharmacology (2003) **28,** 2010–2019, advance online publication, 20 August 2003; doi:10.1038/sj.npp.1300281

Keywords: serotonin transporter; receptor imaging; positron emission tomography; kinetic modeling; [^{18}F](+)-FMe-McN5652; citalopram

INTRODUCTION

Although there is a vast body of evidence that the serotonin transporter (SERT) in the brain is involved in various psychiatric disorders such as depression, anxiety, suicidality, obsessive compulsive disorder, schizophrenia, and others (Heinz *et al*, 1998; Menza *et al*, 1999; Bondy *et al*, 2000; Dahlström *et al*, 2000; Laruelle *et al*, 2000; Saxena *et al*, 2002; Tsai *et al*, 2002), its specific role in different emotional, motivational, and cognitive dysfunctions remains to be elucidated. Owing to the emerging socioeconomic impact of these neuropsychiatric disorders, there is a growing need in developing neuroimaging techniques to evaluate the availability and function of the SERT in the living human brain. Positron emission tomography (PET) as well as single-photon emission tomography (SPECT) enables to visualize the SERT *in vivo* (Hesse *et al*, 2003), whereby PET offers the advantages of higher spatial resolution and the possibility for absolute quantification compared with SPECT.

Although many drugs showing a high *in vitro* binding to the SERT have been used as templates for the development of radioligands for PET, most of them have been found to be unsuitable because of their insufficient selectivity (Brust *et al*, 1999).

In 1992, [^{11}C]McN5652 was introduced as a new radioligand for SERT imaging with PET (Suehiro *et al*, 1992). It has been used for quantification of the SERT in the normal human brain (Szabo *et al*, 1999; Buck *et al*, 2000; Parsey *et al*, 2000; Ikoma *et al*, 2002) and in patients

*Correspondence: Dr P Brust, Institut für Interdisziplinäre Isotopenforschung, Permoserstr. 15, 04318 Leipzig, Germany, Tel: +49 341 235 4013, Fax: +49 341 235 2731, E-mail: brust@iif-leipzig.de
Received 20 February 2003; revised 13 May 2003; accepted 13 June 2003
Online publication: 25 June 2003 at http://www.acnp.org/citations/Npp06250303073/default.pdf

intoxicated with MDMA (McCann *et al*, 1998; Ricaurte *et al*, 2000), with social phobia (Kent *et al*, 2002), major depression (Ichimiya *et al*, 2002), and bipolar disorder (Ichimiya *et al*, 2002). However, its rather high nonspecific binding in the brain and its slow release from the specific binding sites (Szabo *et al*, 1999; Buck *et al*, 2000) promoted the search for alternatives, as is also indicated by some SPECT studies with [^{123}I]-β-CIT which provided opposite results in similar patient populations (ie depression; Malison *et al*, 1998). On the other hand, SERT data obtained by [^{11}C]McN5652/PET (Yamamoto *et al*, 2002) and [^{123}I]-β-CIT/SPECT (Hesse *et al*, 2003) have been very consistent. Thus, there is a necessity to create and make use of sufficient reliable SERT radiopharmaceuticals which should be designed to prevent confounding findings. The ^{11}C-labeled radioligands *N*,*N*-dimethyl-2-(2-amino-4-methoxyphenylthio)benzylamine (DAPP) and *N*,*N*-dimethyl-2-(2-amino-4-cyanophenylthio)benzylamine (DASB) have also been introduced for SERT imaging in humans, and it has been shown that [^{11}C]DASB is superior to [^{11}C]DAPP (Houle *et al*, 2000; Ginovart *et al*, 2001; Meyer *et al*, 2001). Szabo *et al* (2002) have compared [^{11}C]DASB and [^{11}C]McN5652 in baboons, and concluded that both radiotracers were comparably effective in detecting reduced SERT density after MDMA-induced neurotoxicity.

Alternatively, various attempts have been made to synthesize an SERT radioligand labeled with the longer-lived isotope ^{18}F. Karramkam *et al* (2002) synthesized an ^{18}F-labeled derivative of 6-nitroquipazine as a radioligand for the *in vivo* SERT imaging, but concluded that the compound does not have the expected potential for PET imaging. In a preliminary communication, Huang *et al* (2002) reported that [^{18}F]AFM ([^{18}F]2-[2-[(dimethylamino)methyl] thiophenyl]-5-fluoromethyl-phenylamine) is a specific PET radiotracer for the SERT. We have synthesized an ^{18}F-labeled radiotracer for SERT imaging based on (+)-McN5652 (Zessin *et al*, 2001). The replacement of hydrogen by fluorine at the *S*-methyl group of McN5652 reduced the affinity to the 5-HT transporter only slightly and studies with [^{18}F](+)-FMe-McN5652 in rats and pigs revealed that this radiotracer might be suitable for *in vivo* imaging of the SERT in humans (Brust *et al*, 2003; Marjamäki *et al*, 2003). *Ex vivo* autoradiographic studies in rats showed marked accumulation in brain regions with a known high density of the 5-HT transporter such as raphe nuclei, substantia nigra, thalamus, and amygdala. A maximum activity concentration ratio of 9 between brain regions with specific binding (raphe nuclei) and without specific binding (cerebellum) was reached within 3.5 h after tracer administration (Marjamäki *et al*, 2003). First PET studies in pigs revealed that the highest accumulation of [^{18}F](+)-FMe-McN5652 was found in the ventral midbrain, thalamus, olfactory lobe, and pons (Brust *et al*, 2003). A strong inhibition of the specific binding was observed after pretreatment with the selective 5-HT uptake inhibitor citalopram.

The present study was performed to investigate the *in vivo* kinetics of [^{18}F](+)-FMe-McN5652, in order to provide a reliable tool for further clinical neuroimaging SERT studies. Various methods for quantification of the SERT density in pigs were compared.

METHODS

Synthesis of Radiotracers

[^{11}C](+)-McN5652, [^{18}F](+)-FMe-McN5652, and [^{18}F](−)-FMe-McN5652 were synthesized by *S*-methylation or by *S*-fluoromethylation of the corresponding normethyl-McN5652, as previously described (Zessin *et al*, 1999, 2001). Briefly, the thioester precursors were prepared from enantiomerically pure (+)-McN5652 or (−)-McN5652 by *S*-demethylation with sodium amide, followed by conversion of the thiols with acetyl chloride.

The hydrolized thioester precursor and [^{11}C]methyl-iodide were reacted at 40°C for 2 min in dimethyl-formamide. [^{11}C](+)-McN5652 was purified by reversed-phase high-performance liquid chromatography (HPLC). The specific activity of [^{11}C](+)-McN5652 was 37 ± 12 GBq μmol^{-1}.

Molecular modeling calculations were performed with the program package PC Spartan Pro 5.1 (Wavefunction, Inc.) on a PC AMD Athlon 600 MHz (512 MB RAM). Equilibrium geometries of ligands were calculated based on density-functional theory (DFT) (Ziegler, 1991). The Becke–Perdew (BP86) functional with Becke's gradient correction for the local expression of the exchange energy (Becke, 1988) and Perdew's gradient correction for the local expression of the correlation energy (Perdew, 1986) was used. The numerical polarization basis set DN* leading to pBP/DN* model was chosen. The starting conformations of ligands were obtained by force-field calculations using the MMFF94 force field (Halgren, 1996). Charge distribution calculations were performed based on fitting of the electrostatic potential leading to electrostatic charges (Breneman and Wiberg, 1990).

The detailed synthesis of [^{18}F](+)-FMe-McN5652 was described recently (Zessin *et al*, 2001). Briefly, demethylated (+)-McN5652 (prepared from the corresponding thioester precursor) was reacted with [^{18}F]bromofluoromethane (Bergman *et al*, 2001) to yield [^{18}F](+)-FMe-McN5652. The product mixture containing [^{18}F](+)-FMe-McN5652 was purified by reversed-phase HPLC. The radiochemical purity of [^{18}F](+)-FMe-McN5652 was about 95%. The specific activity of [^{18}F](+)-FMe-McN5652 was 34 ± 10 GBq μmol^{-1}. [^{18}F](−)-FMe-McN5652 was prepared in a similar manner, starting from normethyl (−)-McN5652.

Animals and Drugs

All procedures involving animals were carried out according to the 'Principles of laboratory animal care' (NIH publication No. 86-23, revised 1985), and following the German Law on the Protection of Animals. Female pigs (Deutsches Landschwein/Deutsches Edelschwein × Pietrain, 13–17 kg) were used. They were deprived of food, but not of water, for 24 h prior to delivery to the laboratory. Anesthesia was induced initially with midazolam (Dormicum, 1 mg kg^{-1}, i.m.) and ketamine (Curamed, 12 mg kg^{-1}, i.m.).

Citalopram was a kind gift from H Lundbeck A/S (Copenhagen, Denmark). Fluoxetine was kindly provided by Eli Lilly & Company, Inc. (Indianapolis, IN).

Positron Emission Tomography

In all, 28 6-week-old farm-bred female pigs were studied with PET under general anesthesia (0.5% isoflurane in a gas mixture of 70% nitrous oxide and 30% oxygen, via endotracheal tube using a volume-controlled ventilator). Pancuronium was infused at a rate of 0.3 mg kg^{-1} h^{-1}. Blood gases, end-tidal CO_2, and body temperature were continuously monitored. The radiotracer was infused as a smooth bolus into the left jugular vein over 2 min. The applied dose was 242 ± 94 MBq for [^{11}C](+)-McN5652, 274 ± 110 MBq for [^{18}F](+)-FMe-McN5652, and 266 MBq for [^{18}F](−)-FMe-McN5652. The injected total mass of the tracers (determined by HPLC) was 1.85 ± 0.48 μg for [^{11}C](+)-McN5652, 2.28 ± 0.47 μg for [^{18}F](+)-FMe-McN5652, and 1.80 μg for [^{18}F](−)-FMe-McN5652. The radiotracers were prepared for injection in a mixture of ethanol and 0.11 M $NaHCO_3$ (1 : 1 v v^{-1}), and further diluted with saline (1 : 1 v v^{-1}) immediately before injection. The PET scan was started simultaneously with the infusion. Three pigs of the [^{11}C](+)-McN5652 group and five pigs of the [^{18}F](+)-FMe-McN5652 group received an additional i.v. injection (5 mg kg^{-1}) of the 5-HT reuptake inhibitor citalopram before radiotracer infusion. Three pigs of the [^{18}F](+)-FMe-McN5652 group were pretreated with the norepinephrine uptake inhibitor maprotiline (5 mg kg^{-1} i.v.). PET imaging (35 dynamic time frames of length between 0.5 and 10 min, total scan duration: 120 min) was performed with an ECAT EXACT HR+ (CTI/Siemens) scanner, at a spatial resolution (transaxial) of 4–5 mm (Brix *et al*, 1997). Reconstruction of both PET scans was performed using filtered back projection with a Hanning filter (cutoff frequency of 0.5). For attenuation and scatter correction, a transmission scan using three rotating ^{68}Ge rod sources was performed prior to the emission scan. Radioactivity data of selected volumes of interest (VOI) were obtained using a standardized procedure, which was recently described in detail (Brust *et al*, 2003). Briefly, irregular VOIs defined on MR images were aligned to the added PET radioactivity images interactively using an 'in-house' data analysis tool.

During the PET scans, 31–47 discrete arterial blood samples (about 0.2 ml each) were obtained at defined time points starting with the onset of radiotracer infusion, and in intervals between 15 s and 30 min. The samples were immediately stored on ice and centrifuged at 3000*g* for plasma sampling and counting in a γ-counter that was crosscalibrated to the PET camera. The calibration factor was used to calculate absolute values of radioactivity from the counts per minute (cpm) values obtained from the counter. Between six and 11 additional blood samples were obtained for HPLC analysis of plasma metabolites. After centrifugation, 0.5 ml plasma was obtained and precipitated with ethanol (plasma : EtOH = 1 : 1.5 v v^{-1}). Metabolite analysis was carried out by gradient HPLC in the following configuration: Hewlett-Packard 1100 quaternary gradient pump, autosampler (900 μl sample loop; injection volume 500–900 μl), UV detector (λ = 254 nm), all parts of the Hewlett-Packard 1100 system, and a flow scintillation analyzer (150 TR, Canberra Packard) with a PET flow cell (100 μl volume; energy window: 80–1750 keV). The analytes were separated on Merck RP-18e column (Purospher, 125 × 3 mm, 5 μm) at a temperature of 28°C. A binary gradient was chosen at a flow rate of 0.75 ml min^{-1} (0–1 min 23% B, 5–11 min 70% B; total method time: 11 min). Mobile phase A consisted of 0.1 M ammonium formate, pH 7.0. Mobile phase B was MeCN. The metabolite data were fitted to an empiric function, the parameters of which were then used for the correction of the plasma input function.

Data Analysis and Model Description

The general model for the description of the binding of PET ligands *in vivo* to drug-binding sites was introduced by Mintun *et al* (1984). For the analysis of [^{11}C](+)-McN5652 binding to the SERT, only the simplified structures of the one- and two-tissue compartment models (Koeppe *et al*, 1991; Buck *et al*, 2000) were used to describe the binding of the radioligand in the pig brain (Figure 1). In these two compartmental models, the total radiotracer accumulation in the brain regions, *M(t)*, can be described by

$$M(t) = M_t(t) + V_0 C_a(t) \quad (1)$$

$$M(t) = M_f(t) + M_b(t) + V_0 C_a(t) \quad (2)$$

where $M_t(t)$ is the total amount of radiotracer in the brain tissue (one-tissue compartment model, Equation (1)). $M_f(t)$ represents the free and nonspecifically bound radiotracer in the brain tissue and $M_b(t)$ the regional content of the radiotracer specifically bound to the SERT (two-tissue compartment model, Equation (2)).

Following the common notation of Koeppe *et al* (1991), the ordinary differential equations that describe the time courses of radioactivity contents in these models are
one-tissue compartment model:

$$dM_t/dt = K_1 C_a(t) - k_2'' M_t(t) \quad (3)$$

two-tissue compartment model:

$$dM_f/dt = K_1 C_a(t) - k_2' M_f(t) - k_3' M_f(t) + k_4 M_b(t) \quad (4)$$

$$dM_b/dt = k_3' M_f(t) - k_4 M_b(t) \quad (5)$$

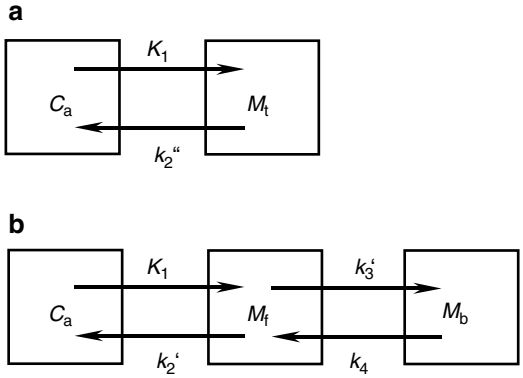

Figure 1 One- (a) and two-tissue compartment models (b) for radiotracer distribution in the porcine brain. C_a, arterial plasma concentration of the radiotracer; M_t, total radiotracer amount in brain tissue; M_f, free and nonspecifically bound amount of the radiotracer; M_b, radiotracer amount specifically bound to the SERT.

K_1 in (ml plasma) (ml tissue)$^{-1}$ min^{-1} is the unidirectional clearance of the ligand from plasma to tissue. $C_a(t)$ is the concentration of parent radioligand in arterial plasma as a function of time t. The rate constants k_2', k_2'', k_3', and k_4 are given in min^{-1}.

The rate constants were estimated by weighted nonlinear least-squares fits to the decay-corrected tissue time–activity curves using the simplex method (Nelder and Mead, 1965).

Distribution volumes (*DV*) were calculated to provide parameter estimates related to binding of the radiotracer to the serotonin transporter. In PET, the total *DV* is the partition ratio between the total concentration of ligand in the tissue and that in plasma which would be attained in a steady-state equilibrium between the two (Cunningham and Lammertsma, 1995). *DV* is given in (ml plasma) (ml tissue)$^{-1}$.

With the one-tissue compartment model, the total distribution volume DV'' is equal to K_1/k_2''. From the region-to-occipital cortex ratio of DV'', the transporter occupancy (in %) was defined as the per cent reduction of the ratio after administration of citalopram, when compared with the ratio at baseline (Farde *et al*, 1997; Kent *et al*, 2002). With the two-tissue compartment model, the total distribution volume DV_t is equal to $K_1/k_2'(1+k_3'/k_4)$ (Koeppe *et al*, 1991).

Furthermore, two parameters more directly related to the ratio B_{max}'/K_D were calculated for the two-tissue compartment model: $f_2\,BP = k_3'/k_4$ and $f_1\,BP = (K_1/k_2') \cdot (k_3'/k_4)$. B_{max}' is the concentration of maximum available receptor sites in competition with endogenous and infused cold ligand. K_D is the aqueous equilibrium ligand-dissociation constant. $BP = B_{max}'/K_D$ is the binding potential and is unitless (Mintun *et al*, 1984). f_1 is the free fraction of the radiotracer in plasma (unitless). f_2 is the free fraction of the radiotracer in tissue and is unitless.

These outcome measures have been given different names in the PET literature. Laruelle *et al* (1994) referred to $f_2\,BP$ as V_3'' and to $f_1\,BP$ as V_3'. Carson *et al* (1997) defined R as $f_2\,BP$ and S as $f_1\,BP$. $f_1\,BP = (K_1/k_2')(k_3'/k_4)$ is also equal to the distribution volume of the specific binding compartment relative to the plasma input, as used by Buck *et al* (2000) in their assessment of methods.

For the estimation of the parameters of the two-tissue compartment model, different parameter constraints were used. These constraints were:

1. the blood volume V_0 fixed at 0.05 (Lin *et al*, 1999);
2. the ratio K_1/k_2' fixed;
3. the ratio K_1/k_2' fixed and a fixed blood volume V_0.

For coupling of K_1 and k_2', the mean values of the regional parameters were used, as estimated after complete blockade of the specific binding to the SERT by pretreatment with citalopram. Goodness of fit of the different models was assessed using the F-test and the Akaike information criterion (AIC) (Akaike, 1974; Hawkins *et al*, 1986). A significant improvement of the fit using model B instead of model A is indicated by F-values of >4.15 ($P<0.05$) or AIC (model B) $<$ AIC (model A).

The data are mean values $\pm$ standard deviation (SD). The coefficient of variation (COV) was calculated by mean/SD $\times$ 100. The *t*-test was used to evaluate significant differences.

RESULTS

Coronal PET images of three piglet brains acquired at 60–70 min post-radiotracer injection are presented in Figure 2. The highest accumulation of [^{18}F](+)-FMe-McN5652 was found in the ventral midbrain area (Figure 2a, c, e) injection of the SERT inhibitor citalopram clearly inhibited this binding, and results in a rather uniform tracer distribution (Figure 2b). The calculated transporter occupancy by citalopram was 95% ([^{11}C](+)-McN5652) and 97% ([^{18}F](+)-FMe-McN5652) in the midbrain. A similar distribution was found for the inactive enantiomer [^{18}F](−)-FMe-McN5652 (Figure 2d). Preinjection of the norepinephrine uptake inhibitor maprotiline was without effect (Figure 2f). The normalized metabolite-corrected arterial plasma input functions of [^{18}F](+)-FMe-McN5652 without and with preinjection of citalopram are shown in Figure 3a, and compared with the corresponding input functions of the ^{11}C-labeled derivative (Figure 3b). There are no significant differences between both radiotracers. To test this assumption, the area under the curve and the peak radioactivity levels of both input functions were compared using the *t*-test. Preinjection of citalopram resulted in an increase of both tracer input functions throughout the whole study. However, the estimated rate constant for blood–brain transfer (K_1) remained unchanged (98% of

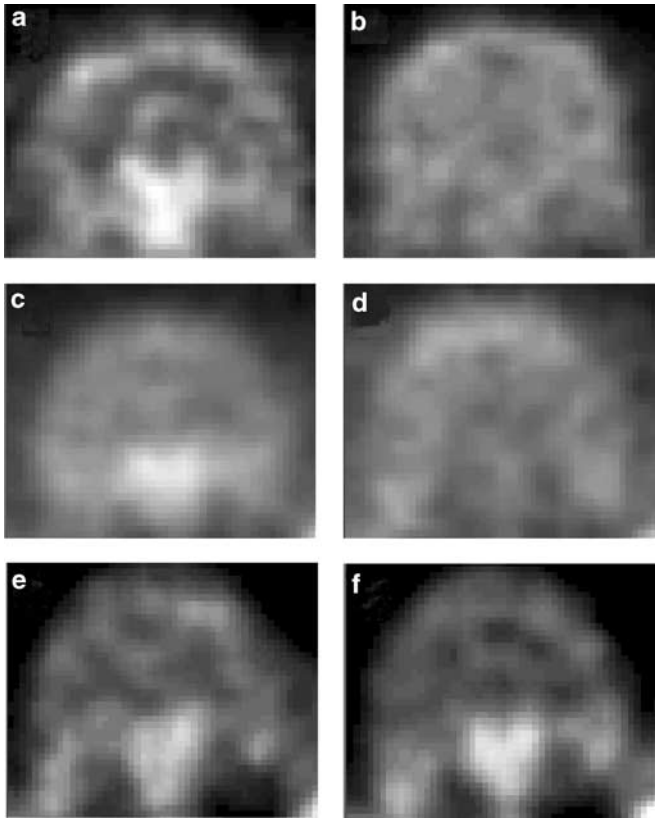

Figure 2 Coronal PET images of three individual piglet brains showing the distribution of [^{18}F](+)-FMe-McN5652 before (a,c,e), and after preinjection of citalopram (b) or maprotiline (f), and the distribution of the inactive enantiomer [^{18}F](−)-FMe-McN5652 (d). The PET images were acquired at 60–70 min post-radiotracer injection. The activity scale ranges from dark (low) to white (high).

control). The fitted blood volume decreased by about 17% ($p \leqslant 0.10$).

In separate plasma samples, the metabolism of both radiotracers was investigated by HPLC. Figure 4 shows the relative amounts of the parent compounds in the samples in dependency on the time of injection. The overlapping of the two functions indicates that the rate of peripheral metabolism of both radiotracers is nearly identical. As can be seen from chromatograms obtained 12 min after radiotracer injection (Figure 5), even the metabolite profiles measured on the HPLC system are similar. Occasionally, small negligible amounts of a lipophilic metabolite were detectable for both radioligands although the relative amounts were higher for [^{11}C](+)-McN5652 (1–2% at 20 min, 3–4% at 60 min) than for [^{18}F](+)-FMe-McN5652 (<1% at 20 min, 2–3% at 120 min). The peripheral radiotracer metabolism was unchanged after preinjection of citalopram or maprotiline (data not shown).

Various compartmental models were used for quantification of the brain uptake of [^{11}C](+)-McN5652 and [^{18}F](+)-FMe-McN5652 (Figure 1). The coefficient of variation (COV) of the calculated binding parameter (DV'') was lowest for the one-tissue compartment model (^{11}C: 69.9%, ^{18}F: 14.5% in midbrain), but the F-test and calculation of the Akaike information criterion revealed that any of the chosen two-tissue compartment models was better than the one-tissue compartment model. Typical examples of brain time–activity curves in the ventral midbrain, striatum, and temporal and occipital cortex obtained with both radiotracers after an i.v. injection of about 200 MBq into a single female piglet are shown in Figure 6. The solid lines in this figure represent the model fits using an unconstrained two-tissue compartment model. Table 1 shows the calculated rate constants according to this model. The ^{18}F-labeled derivative has an about 30% higher influx rate constant, K_1, with a 50% lower COV than the ^{11}C-labeled compound. The regional influx rate constants of both radiotracers are strongly correlated ($r = 0.780$, $p < 0.01$). The clearance rate constant k_2' of [^{18}F](+)-FMe-McN5652 is about two-fold higher than that of [^{11}C](+)-McN5652, indicating a faster kinetics of the former compound. In all investigated regions, the goodness of the fits was significantly improved if a two-tissue

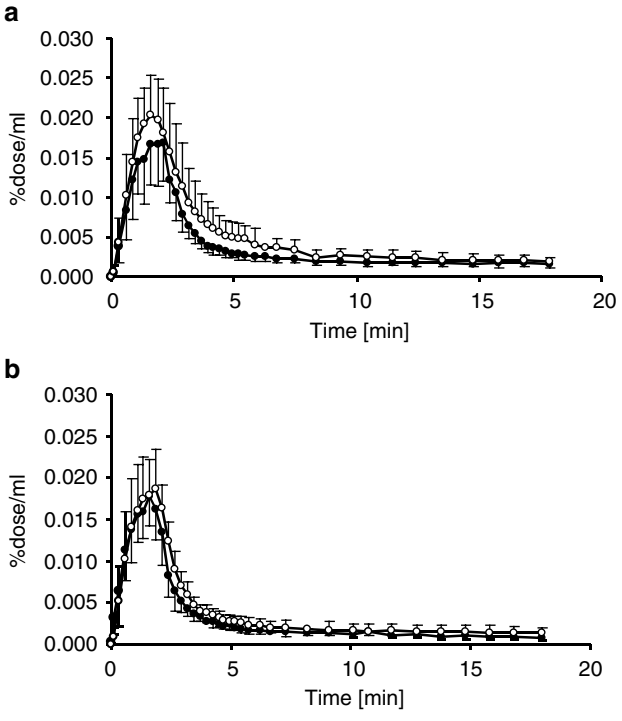

Figure 3 Normalized metabolite-corrected arterial plasma input functions of [^{18}F](+)-FMe-McN5652 (a) and [^{11}C](+)- McN5652 (b) without and with preinjection of citalopram (5 mg kg^{-1}). (a) ● – [^{18}F](+)-FMe-McN5652, ○ – [^{18}F](+)-FMe-McN5652 + citalopram; (b) ● – [^{11}C](+)-McN5652, ○ – [^{18}F](+)-McN5652 + citalopram.

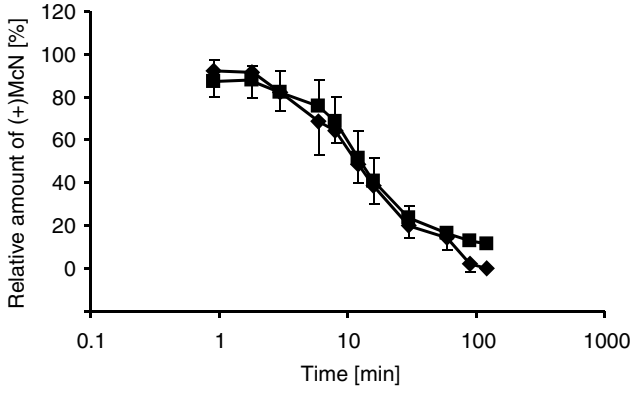

Figure 4 Relative amounts of [^{18}F](+)-FMe-McN5652 (■) or [^{11}C](+)- McN5652 (◆) in porcine plasma, at various time points after i.v. injection.

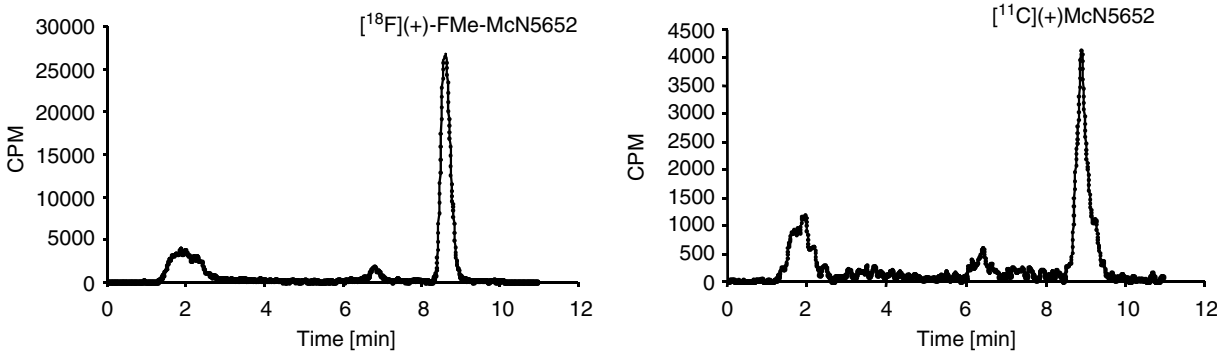

Figure 5 Radiochromatograms of porcine plasma obtained 12 min after i.v. injection of [^{18}F](+)-FMe-McN5652 (left) or [^{11}C](+)- McN5652 (right).

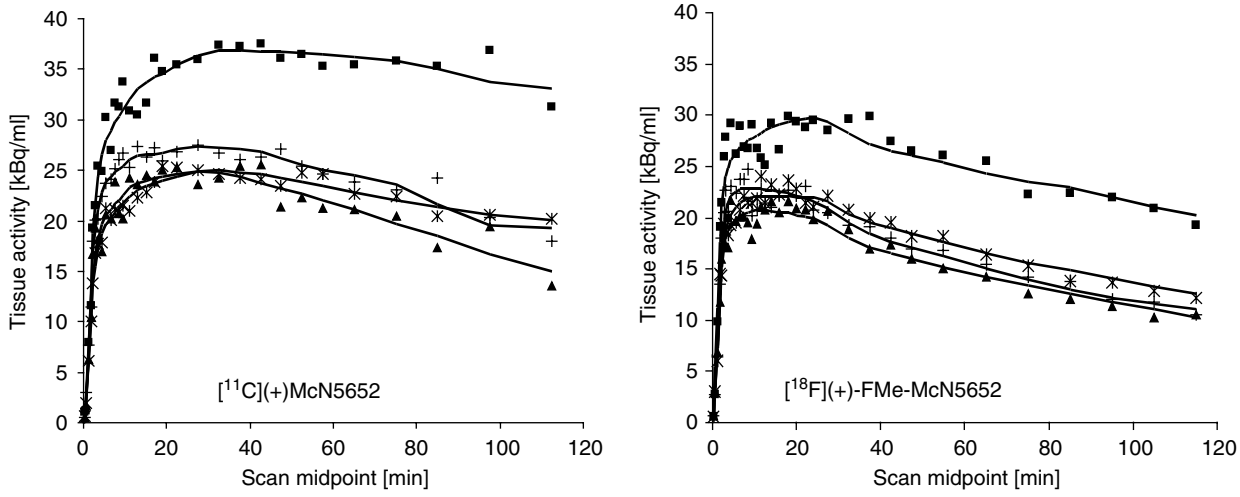

Figure 6 Kinetics of [^{11}C](+)-McN5652 (left), [^{18}F](+)-FMe-McN5652 (right) in the ventral midbrain (■), striatum (+), temporal (*), and occipital (▲) cortex of a single female piglet, after injection of about 200 MBq of the radiotracer. The solid lines represent the fit results according to a two-tissue compartment model without constraints.

Table 1 Comparison of the Blood–Brain Transfer Rate Constant K_1, the Clearance Rate Constant k_2', the Ratio k_3'/k_4 (which is Proportional to the Binding Potential) and the Region-to-Occipital Cortex Ratio of k_3'/k_4 for [^{11}C](+)-McN5652 and [^{18}F](+)-FMe-McN5652 in Female Piglets Estimated Using an Unconstrained Two-compartment Model

	[^{11}C](+)-McN5652 ($n=7$)				[^{18}F](+)-FMe-McN5652 ($n=9$)			
	K_1 (ml ml^{-1} min^{-1})	k_2' (min^{-1})	k_3'/k_4	Ratio	K_1 (ml ml^{-1} min^{-1})	k_2' (min^{-1})	k_3'/k_4	Ratio
Midbrain	0.336 ± 0.094	0.027 ± 0.006	8.28 ± 3.95	1.83	0.408 ± 0.063	0.047 ± 0.015	2.75 ± 0.61	2.22
Striatum	0.365 ± 0.091	0.033 ± 0.009	5.56 ± 2.36	1.23	0.413 ± 0.057	0.059 ± 0.012	1.63 ± 0.32	1.32
Temp. cortex	0.298 ± 0.086	0.030 ± 0.008	5.44 ± 2.19	1.20	0.403 ± 0.058	0.055 ± 0.012	2.16 ± 0.78	1.74
Occip. cortex	0.284 ± 0.108	0.033 ± 0.009	4.53 ± 2.30	1.00	0.409 ± 0.051	0.058 ± 0.012	1.24 ± 0.35	1.00

compartment model was chosen instead of a one-tissue compartment model ($F > 45.1$ for [^{11}C](+)-McN5652 and $F > 76.4$ for [^{18}F](+)-FMe-McN5652). Table 1 compares the ratio k_3'/k_4, which is the parameter closest to specific radiotracer binding. The region-to-occipital cortex ratio of this parameter for [^{18}F](+)-FMe-McN5652 is higher than for the ^{11}C-labeled derivative in all regions studied. Various binding parameters of the one- and two-tissue compartmental models estimated in the porcine midbrain and in the occipital cortex are shown in Table 2. Generally, the absolute values of these parameters and also the COVs are much higher for [^{11}C](+)-McN5652 than for [^{18}F](+)-FMe-McN5652. If constrained models were used, the region-to-occipital cortex ratios increased by more than a factor of 10. However, this was accompanied by a considerable increase (about a factor of 2–3) of the COVs (data not shown).

The binding parameter $f_1 BP$ (obtained from the unconstrained fit) was found to be the one that correlates best with the SERT density, as determined by *in vitro* autoradiography with [^{3}H]citalopram on the porcine brain (Cumming *et al*, 2001; Kretzschmar *et al*, 2003). This highly significant correlation is shown in Figure 7 for both radiotracers.

DISCUSSION

The results of PET studies performed in piglets indicate that [^{18}F](+)-FMe-McN5652 is a suitable radioligand for imaging serotonin transporter sites in the human brain. This conclusion is derived from the following observations:

(1) Compared to the recently introduced SERT radioligand [^{11}C](+)-McN5652, it shows the same characteristic pattern for the distribution of serotonin uptake sites.
(2) The accumulation in the midbrain, an area of high SERT density, can be blocked by the specific SERT inhibitor citalopram, but not by the norepinephrine transport inhibitor maprotiline.
(3) The kinetics and metabolism of [^{18}F](+)-FMe-McN5652 are similar to those of the ^{11}C-labeled congener.
(4) The regional binding parameters of [^{11}C](+)-McN5652 and [^{18}F](+)-FMe-McN5652 are highly correlated among each other and with the SERT density, as determined by *in vitro* binding of [^{3}H]citalopram.

To date, neuroimaging techniques (PET, SPECT) represent valid approaches to determine neurotransmitter changes in the living human brain. Various radiolabeled

Table 2 Comparison of Averaged Parameters Related to SERT Density Estimated in Porcine Midbrain and Occipital Cortex Using One- (A) and Two-tissue Compartment Model (B)

		[^{11}C](+)-McN5652 ($n=7$)			[^{18}F](+)-FMe-McN5652 ($n=9$)		
Parameter	**Model**	**Midbrain**	**Occ. Cortex**	**Ratio**	**Midbrain**	**Occ. Cortex**	**Ratio**
DV″	A (Mean)	68.5	20.5	3.3	19.9	8.9	2.2
	%COV	69.9	49.7		14.5	16.9	
DV_t	B (Mean)	144.4	36.3	4.0	34.8	14.8	2.4
	%COV	74.7	61.8		25.4	19.0	
f_1 *BP*	B (Mean)	131.0	27.1	4.8	24.2	7.9	3.1
	%COV	79.4	76.5		23.2	34.0	
f_2 *BP*	B (Mean)	8.3	4.5	1.8	2.8	1.2	2.3
	%COV	47.6	50.9		22.0	28.0	

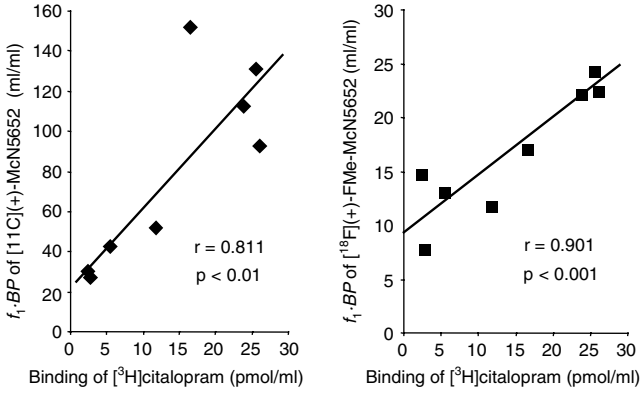

Figure 7 Correlation between the specific binding of [^{3}H]citalopram at the porcine brain *in vitro* ($n=3$, data from Cumming *et al* (2001) and Kretzschmar *et al* (2003)) and the binding parameter f_1 *BP* (without constraints) of [^{11}C](+)-McN5652 (left) or [^{18}F](+)-FMe-McN5652 (right). Data are means of the values measured in various brain regions (midbrain, thalamus, colliculi, hippocampus, striatum, basal cortex, frontal cortex, cerebellum).

ligands specific for different types of receptors and transporters have been developed to measure abnormalities in the binding potentials of distinct receptors in neuropsychiatric disorders. However, much remains unclear about the function and disturbed function of each transmitter system, or of the complex transmitter network itself. The serotonin transporter is one of the sites of major interest in brain neurochemical research, because modern psychopharmaceuticals, that is the selective serotonin reuptake inhibitors (SSRI), act effectively on these structures in depression, anxiety, social phobia, obsessive–compulsive disorder, and post-traumatic stress (Ables and Baughman, 2003). Owing to the socioeconomic burden of neuropsychiatric diseases (Lopez and Murray, 1998), there is an increasing demand not only for a reliable research, but also for a diagnostic tool to image the pathophysiology of these disorders *in vivo*.

Recently, we have described the synthesis of [^{18}F](+)-FMe-McN5652 as a potential PET radioligand for the serotonin transporter (Zessin *et al*, 2001). Compared to [^{11}C](+)-McN5652 ($K_i=0.72$ nM), it has a lower affinity of $K_i=2.3$ nM, which in turn leads to a faster equilibration in PET studies. As pointed out by Halldin *et al* (2002), the applicability of many previously introduced PET radioligands for the serotonin transporter suffered from too small K_i values, and a tracer with a K_i of 1.96 nM was proposed as well suited for *in vivo* quantification. The increased counting statistics at later times of the PET scan favors further the ^{18}F-labeled McN5652 over the ^{11}C analogue. We have shown by *in vitro* and *ex vivo* autoradiography that [^{18}F](+)-FMe-McN5652 selectively labels the serotonin transporter in the brain of rats and pigs. There was a strong correlation between the specific *in vitro* binding of [^{18}F]FMe-McN and [^{3}H]citalopram in the various porcine brain regions (Kretzschmar *et al*, 2003). The maximum target–nontarget ratio *in vitro* was 21 in rats and 15 in pigs (Kretzschmar *et al*, 2003). *Ex vivo* autoradiography in rats revealed a ratio of 9 in the raphe nuclei (Marjamäki *et al*, 2003). PET studies performed in pigs revealed a midbrain–occipital cortex ratio of about 2 for both radioligands [^{18}F](+)-FMe-McN5652 and [^{11}C](+)-McN5652 (Brust *et al*, 2003). However, such target-to-nontarget uptake ratios are not a precise measure for the SERT density, because neither a full kinetic equilibrium nor a 'pseudo-equilibrium' has been reached during these studies.

The present study demonstrates that citalopram is able to block most of the sites (97%) available for binding of [^{18}F](+)-FMe-McN5652. Citalopram is a very selective SERT inhibitor with no effects on dopaminergic or noradrenergic uptake systems (Christensen *et al*, 1977; Hyttel, 1977). A usual problem with giving massive doses of i.v. SERT inhibitors (in our case: 5 mg kg^{-1}) is that one cannot be certain that regional cerebral blood flow was not affected. Clomipramine (0.15 mg kg^{-1}) administered into humans caused a selective decrease of CBF in the dorsomedial nucleus of the thalamus (Smith and Geday, 2001). Citalopram, given to patients with social phobia, also elicited a blood flow decrease in selected brain regions (Furmark *et al*, 2002). In rats, citalopram (10 mg kg^{-1}) reduced the CBF in nine of 27 brain areas analyzed.

Concomitantly, the glucose utilization was decreased, and it was suggested that the blood flow reduction may be entirely explained by the secondary effects of depressed metabolic demand induced by citalopram (McBean *et al*, 1999). In our study, only small blood flow changes are expected. The cerebral blood volume estimated using compartmental modeling was only slightly decreased and the flow-dependent blood–brain transfer (K_1) was unchanged. Therefore, the decreased radiotracer accumulation observed after preinjection of citalopram (Figure 2b) should mainly be caused by blockade of the SERT-binding sites.

Special consideration was given to the metabolism of [^{18}F](+)-FMe-McN5652 in this paper, since hydrolytic instabilities have been reported for several [^{18}F]fluoromethyl compounds (Coenen *et al*, 1986; Petric *et al*, 1999). The radiotracer was prepared in a mixture of ethanol and 0.11 M sodium bicarbonate solution (1 : 1 v v^{-1}). This solvent mixture has been proven to provide stability for a period of at least 120 min (Zessin *et al*, 2001). It has a purity of >95%. The remaining <5% included only polar products. A further 1 : 1 dilution with saline immediately prior to injection did not cause a measurable degradation of the radiotracer. Lipophilic radiolabeled metabolites were only detectable at later scan times, and included less than 5% of the total radiotracer amount.

After injection, a nearly identical metabolic pattern was observed for the ^{18}F-labeled and for the ^{11}C-labeled derivative. The rates of peripheral metabolism and the resulting metabolites are similar. Although the exact identity of the metabolites is still unknown, the early appearance of very polar metabolites with a similar retention time and in a similar relative amount indicates cleavage of the *S*-[^{11}C]methyl and the *S*-[^{18}F]fluoromethyl bond, respectively, as an early step of the metabolism for both radiotracers. At a later time, defluorination of [^{18}F](+)-FMe-McN5652 occurs, as can be seen by accumulation of radioactivity in the skull in PET images acquired between 180 and 240 min p.i. (data not shown). The rate of radiotracer metabolism in the piglet is comparable to that in humans. Szabo *et al* (1999) have found 14 ± 6% of the unmetabolized [^{11}C](+)-McN5652 in human plasma at 60 min p.i. In our study, we have determined an identical value (14.1 ± 5.8%) at this time. For the ^{18}F-labeled derivative, a slightly higher value was found (16.1 ± 3.3%).

Based on the metabolite-corrected arterial plasma input functions, we have calculated parameters related to the blood–brain transfer of the radioligands, and those related to the binding to the SERT. K_1, which describes the tracer uptake across the blood–brain barrier, is about 20–30% higher for [^{18}F](+)-FMe-McN5652 than for [^{11}C](+)-McN5652. This should be due to a higher extraction of the ^{18}F-labeled radiotracer, because the cerebral blood flow is expected to be similar for both radiotracer studies. A higher extraction favors the use of [^{18}F](+)-FMe-McN5652. This was not caused by lipophilicity differences. [^{18}F](+)-FMe-McN5652 and [^{11}C](+)-McN5652 show almost identical lipid solubilities, which was confirmed by measurements of reversed-phase HPLC retention times (see Figure 5) and by ACD molecular modeling calculations which provided a log *D* of 3.14 for (+)-McN5652 and 3.10 for (+)-FMe-McN5652. We suggest that a faster exchange of the free tracer with the blood platelets (because of the lower SERT-binding affinity) is the reason for the higher extraction of [^{18}F](+)-FMe-McN5652. The clearance rate constant k_2' is about 80–100% higher for the ^{18}F-labeled tracer, indicating a faster kinetics of this compound as has been mentioned recently (Brust *et al*, 2003). The exchange of the methylthio group by the fluoromethylthio moiety leads to changes in the charge density. The hydrogen–fluorine exchange results in a shift of the negative charge center from sulfur to the fluorine atom. Furthermore, the calculated dipole moment increased from 1.64 for (+)-McN5652 to 2.25 for (+)-FMe-McN5652. This difference of the charge density may be a reason for the higher clearance rate of [^{18}F](+)-FMe-McN5652.

Regarding the analysis model of [^{11}C](+)-McN5652, some groups recommended the one-tissue compartment model (Szabo *et al*, 1999; Parsey *et al*, 2000), and others the two-tissue compartment model (Buck *et al*, 2000) or a graphical method with a reference tissue input function (Buck *et al*, 2000; Ikoma *et al*, 2002). The various parameter estimates obtained from these models contain a similar amount of information on serotonin transporters. However, none of them reflects the SERT density in a fully quantitative manner (Buck *et al*, 2000). The parameter that is expected to come closest to the binding potential *BP* (Mintun *et al*, 1984) is the k_3'/k_4 ratio ($=f_2\,BP$). However, the direct estimation of k_3' and k_4 is very sensitive to noise, which associates high errors with them (Cunningham and Lammertsma, 1995). Also, in our study with [^{11}C](+)-McN5652, the coefficient of variation of $f_2\,BP$ in various regions was between 40 and 110%. Having the same length of the study (120 min), it was only about half of that for [^{18}F](+)-FMe-McN5652. The data obtained for both radiotracers show high 'nonspecific' binding even in regions with very low SERT density such as the cerebellum or occipital cortex, which is disadvantageous for quantification and sensitivity. The binding parameter $f_2\,BP$ of [^{11}C](+)-McN5652 in high-density regions was about a factor 3.4 greater than in low-density regions. For [^{18}F](+)-FMe-McN5652, it was only a factor of 2.6. The difference between both tracers is even larger if DV_t is compared. In a previous study, we have estimated the specific binding from the difference in tracer uptake at later scan times between a region and the occipital cortex, assuming negligible specific binding in the latter. The data indicated a higher specific binding for [^{18}F](+)-FMe-McN5652 than for [^{11}C](+)-McN5652. However, the estimation was biased because no pseudoequilibrium was reached for either of the tracers. The estimation of $f_2\,BP$ or of DV_t after bolus injection is independent of an equilibrium state, and therefore a better estimate of the specific binding. The discrepancy between both studies may have been caused by the faster kinetics of [^{18}F](+)-FMe-McN5652 compared to [^{11}C](+)-McN5652. Hence, the parameter estimates of [^{18}F](+)-FMe-McN5652 should be less biased than those of [^{11}C](+)-McN5652.

The highest binding potential for the recently introduced [^{11}C]DASB (Houle *et al*, 2000), calculated with the ratio method, was observed in the hypothalamus (Ginovart *et al*, 2001). The estimated value (2.5) is similar to $f_2\,BP$ ($R_v = 2.42$) obtained in the human thalamus using [^{11}C](+)McN5652 (Buck *et al*, 2000), and similar to the value obtained for [^{18}F](+)-FMe-McN5652 in the midbrain in this study (2.8), although in humans a lower value for the

latter may be expected. Compared to ^{11}C-labeled radiotracers, [^{18}F](+)-FMe-McN5652 may be of logistic advantage for those clinical PET users who depend on the transport of radiotracers to their site from external sources. Besides [^{18}F]AFM, for which only preliminary data exist (Huang *et al*, 2002), [^{18}F](+)-FMe-McN5652 is at the moment the only ^{18}F-labeled radioligand that is available for SERT imaging with PET.

In conclusion, we have shown that [^{18}F](+)-FMe-McN5652 can be used to visualize and quantify the SERT density in the porcine brain. The results with various kinetic modeling approaches in a direct comparison of [^{11}C](+)McN5652 and [^{18}F](+)-FMe-McN5652 reveal a higher specific binding of [^{11}C](+)McN5652, but a lower reliability of the derived binding parameters. [^{18}F](+)-FMe-McN5652 may be alternatively used for PET imaging of the SERT in the human brain, but still has limitations in studies that require full quantification. The longer half-life of [^{18}F](+)-FMe-McN5652 compared to the [^{11}C]-labeled analogue enables the use of the former substance in clinical trials or settings far from a fast access to the cyclotron unit.

ACKNOWLEDGEMENTS

We thank the cyclotron staff of the Rossendorf PET Center for providing [^{11}C]carbon dioxide and [^{18}F]fluoride. We also thank U Lenkeit, H Kasper, and N Dohn for technical assistance. This study was supported in part by a grant of DFG (STE 601/8-1). R Hinz is with a DFG research grant (Geschäftszeichen HI 769/1-1).

REFERENCES

Ables AZ, Baughman III OL (2003). Antidepressants: update on new agents and indications. *Am Famicians Phys* **67**: 547–554.

Akaike H (1974). A new look at the statistical model identification. *IEEE Trans Automat Control* **AC19**: 716–723.

Becke AD (1988). Density-functional exchange-energy approximation with correct asymptotic behavior. *Phys Rev A* **38**: 3098–3100.

Bergman J, Eskola O, Lehikoinen P, Solin O (2001). Automated synthesis and purification of [^{18}F]bromofluoromethane at high specific radioactivity. *Appl Radiat Isot* **54**: 927–933.

Bondy B, Erfurth A, de Jonge S, Kruger M, Meyer H (2000). Possible association of the short allele of the serotonin transporter promoter gene polymorphism (5-HTTLPR) with violent suicide. *Mol Psychiatry* **5**: 193–195.

Breneman CM, Wiberg KB (1990). Determining atom-centered monopoles from molecular electrostatic potentials. The need for high sampling density in formamide conformational analysis. *J Comput Chem* **11**: 361–373.

Brix G, Doll J, Bellemann ME, Trojan H, Haberkorn U, Schmidlin P *et al* (1997). Use of scanner characteristics in iterative image reconstruction for high-resolution positron emission tomography studies of small animals. *Eur J Nucl Med* **24**: 779–786.

Brust P, Scheffel U, Szabo Z (1999). Radioligands for the study of the 5-HT transporter *in vivo*. *IDrugs* **2**: 129–145.

Brust P, Zessin J, Kuwabara H, Pawelke B, Kretzschmar M, Hinz R *et al* (2003). Positron emission tomography imaging of the serotonin transporter in the pig brain using [^{11}C](+)-McN5652 and S-([^{18}F]fluoromethyl)-(+)-McN5652. *Synapse* **47**: 143–151.

Buck A, Gucker PM, Schönbächler RD, Argoni M, Kneifel S, Vollenweider FX *et al* (2000). Evaluation of serotonergic transporters using PET and [^{11}C](+)-McN-5652: assessment of methods. *J Cereb Blood Flow Metab* **20**: 253–262.

Carson RE, Breier A, Debartolomeis A, Saunders RC, Su TP, Schmall B *et al* (1997). Quantification of amphetamine-induced changes in C-11 raclopride binding with continuous infusion. *J Cereb Blood Flow Metab* **17**: 437–447.

Christensen AV, Fjalland B, Pedersen V, Danneskiold-Samsoe P, Svendsen O (1977). Pharmacology of a new phthalane (Lu 10-171), with specific 5-HT uptake inhibiting properties. *Eur J Pharmacol* **41**: 153–162.

Coenen HH, Colosimo M, Schüller M, Stöcklin G (1986). Preparation of n.c.a. [^{18}F]CH_2BrF via aminopolyether supported nucleophilic substitution. *J Labelled Compd Radiopharm* **23**: 587–595.

Cumming P, Kretzschmar M, Brust P, Smith DF (2001). Quantitative radioluminography of serotonin uptake sites in the porcine brain. *Synapse* **39**: 351–355.

Cunningham VJ, Lammertsma AA (1995). Radioligand studies in brain: kinetic analysis of PET data. *Med Chem Res* **5**: 79–96.

Dahlström M, Ahonen A, Ebeling H, Torniainen P, Heikkila J, Moilanen I (2000). Elevated hypothalamic/midbrain serotonin (monoamine) transporter availability in depressive drug-naive children and adolescents. *Mol Psychiatry* **5**: 514–522.

Farde L, Ginovart N, Ito H, Lundkvist C, Pike VW, McCarron JA *et al* (1997). PET-characterization of carbonyl-c-11 WAY-100635 binding to 5-HT1a receptors in the primate brain. *Psychopharmacology (Berl)* **133**: 196–202.

Furmark T, Tillfors M, Marteinsdottir I, Fischer H, Pissiota A, Langstrom B *et al* (2002). Common changes in cerebral blood flow in patients with social phobia treated with citalopram or cognitive-behavioral therapy. *Arch Gen Psychiatry* **59**: 425–433.

Ginovart N, Wilson AA, Meyer JH, Hussey D, Houle S (2001). Positron emission tomography quantification of [^{11}C]-DASB binding to the human serotonin transporter: modeling strategies. *J Cereb Blood Flow Metab* **21**: 1342–1353.

Halgren TA (1996). Merck molecular force field. I. Basis, form, scope, parameterization, and performance of MMFF94. *J Comput Chem* **17**: 490–519.

Halldin C, Tarkiainen J, Sovago J, Vercouillie J, Gulyas B, Guilloteau D *et al* (2002). [^{11}C]DADAM – a fast equilibrium PET radioligand for the serotonin transporter. *Neuroimage* **16**: S3.

Hawkins RA, Phelps ME, Huang SC (1986). Effects of temporal sampling, glucose metabolic rates, and disruptions of the blood–brain barrier on the FDG model with and without a vascular compartment: studies in human brain tumors with PET. *J Cereb Blood Flow Metab* **6**: 170–183.

Heinz A, Ragan P, Jones DW, Hommer D, Williams W, Knable MB *et al* (1998). Reduced central serotonin transporters in alcoholism. *Am J Psychiatry* **155**: 1544–1549.

Hesse S, Barthel H, Murai T, Müller U, Müller D, Seese A *et al* (2003). Is correction for age necessary in neuroimaging studies of the central serotonin transporter? *Eur J Nucl Med Mol Imaging* **30**: 427–430.

Houle S, Ginovart N, Hussey D, Meyer JH, Wilson AA (2000). Imaging the serotonin transporter with positron emission tomography: initial human studies with [^{11}C]DAPP and [^{11}C]DASB. *Eur J Nucl Med* **27**: 1719–1722.

Huang Y, Hwang D-R, Narendran R, Talbot PS, Bae SA, Zhu Z *et al* (2002). [F-18]AFM is a specific PET radiotracer for the serotonin transporters: comparison with [C-11]AFM. *Neuroimage* **16**: S2.

Hyttel J (1977). Neurochemical characterization of a new potent and selective serotonin uptake inhibitor: Lu 10-171. *Psychopharmacology (Berl)* **51**: 225–233.

Ichimiya T, Suhara T, Sudo Y, Okubo Y, Nakayama K, Nankai M *et al* (2002). Serotonin transporter binding in patients with mood disorders: a PET study with [^{11}C](+)McN5652. *Biol Psychiatry* **51**: 715–722.

Ikoma Y, Suhara T, Toyama H, Ichimiya T, Takano A, Sudo Y *et al* (2002). Quantitative analysis for estimating binding potential of

the brain serotonin transporter with [^{11}C] McN5652. *J Cereb Blood Flow Metab* **22**: 490–501.

Karramkam M, Dolle F, Valette H, Besret L, Bramoulle Y, Hinnen F *et al* (2002). Synthesis of a fluorine-18-labelled derivative of 6-nitroquipazine, as a radioligand for the *in vivo* serotonin transporter imaging with PET. *Bioorg Med Chem* **10**: 2611–2623.

Kent JM, Coplan JD, Lombardo I, Hwang DR, Huang Y, Mawlawi O *et al* (2002). Occupancy of brain serotonin transporters during treatment with paroxetine in patients with social phobia: a positron emission tomography study with [^{11}C]McN 5652. *Psychopharmacology (Berl)* **164**: 341–348.

Koeppe RA, Holthoff VA, Frey KA, Kilbourn MR, Kuhl DE (1991). Compartmental analysis of [^{11}C]flumazenil kinetics for the estimation of ligand transport rate and receptor distribution using positron emission tomography. *J Cereb Blood Flow Metab* **11**: 735–744.

Kretzschmar M, Brust P, Zessin J, Cumming P, Bergmann R, Johannsen B (2003). Autoradiographic imaging of the serotonin transporter in the brain of rats and pigs using *S*-([^{18}F]fluoromethyl)-(+)-McN565. *Eur J Neuropsychopharmacol* **13**: (in press).

Laruelle M, Abi-Dargham A, van Dyck C, Gil R, D'Souza DC, Krystal J *et al* (2000). Dopamine and serotonin transporters in patients with schizophrenia: an imaging study with [^{123}]I beta-CIT. *Biol Psychiatry* **47**: 371–379.

Laruelle M, van Dyck C, Abi-Dargham A, Zea-Ponce Y, Zoghbi SS, Charney DS *et al* (1994). Compartmental modeling of iodine-123-iodobenzofuran binding to dopamine D2 receptors in healthy subjects. *J Nucl Med* **35**: 743–754.

Lin W, Celik A, Paczynski RP (1999). Regional cerebral blood volume: a comparison of the dynamic imaging and the steady state methods. *J Magn Reson Imaging* **9**: 44–52.

Lopez AD, Murray CC (1998). The global burden of disease, 1990–2020. *Nat Med* **4**: 1241–1243.

Malison RT, Price LH, Berman R, van Dyck CH, Pelton GH, Carpenter L *et al* (1998). Reduced brain serotonin transporter availability in major depression as measured by [^{123}I]-2 beta-carbomethoxy-3 beta-(4-iodophenyl)tropane and single photon emission computed tomography. *Biol Psychiatry* **44**: 1090–1098.

Marjamäki P, Zessin J, Eskola O, Grönroos T, Haaparanta M, Bergman J *et al* (2003). *S*-[^{18}F]fluoromethyl-(+)-McN5652, a PET tracer for the serotonin transporter: evaluation in rats. *Synapse* **47**: 45–53.

McBean DE, Ritchie IM, Olverman HJ, Kelly PA (1999). Effects of the specific serotonin reuptake inhibitor, citalopram, upon local cerebral blood flow and glucose utilisation in the rat. *Brain Res* **847**: 80–84.

McCann UD, Szabo Z, Scheffel U, Dannals RF, Ricaurte GA (1998). Positron emission tomographic evidence of toxic effect of MDMA ('Ecstasy') on brain serotonin neurons in human beings. *Lancet* **352**: 1433–1437.

Menza MA, Palermo B, DiPaola R, Sage JI, Ricketts MH (1999). Depression and anxiety in Parkinson's disease: possible effect of genetic variation in the serotonin transporter. *J Geriatr Psychiatry Neurol* **12**: 49–52.

Meyer JH, Wilson AA, Ginovart N, Goulding V, Hussey D, Hood K *et al* (2001). Occupancy of serotonin transporters by paroxetine and citalopram during treatment of depression: a [^{11}C]DASB PET imaging study. *Am J Psychiatry* **158**: 1843–1849.

Mintun MA, Raichle ME, Kilbourn MR, Wooten GF, Welch MJ (1984). A quantitative model for the *in vivo* assessment of drug binding sites with positron emission tomography. *Ann Neurol* **15**: 217–227.

Nelder JA, Mead R (1965). A simplex method for function minimization. *Comput J* **7**: 308–313.

Parsey RV, Kegeles LS, Hwang DR, Simpson N, Abi-Dargham A, Mawlawi O *et al* (2000). *In vivo* quantification of brain serotonin transporters in humans using [^{11}C]McN 5652. *J Nucl Med* **41**: 1465–1477.

Perdew JP (1986). Density-functional approximation for the correlation energy of the inhomogenous electron gas. *Phys Rev B* **33**: 8822–8824.

Petric A, Barrio JR, Namavari M, Huang SC, Satyamurthy N (1999). Synthesis of 3b-(4-[^{18}F]fluoromethylphenyl)- and 3b-(2-[^{18}F]fluoromethylphenyl)tropane-2b-carboxylic acid methyl esters: new ligands for mapping brain dopamine transporter with positron emission tomography. *Nucl Med Biol* **26**: 529–535.

Ricaurte GA, McCann UD, Szabo Z, Scheffel U (2000). Toxicodynamics and long-term toxicity of the recreational drug, 3, 4-methylenedioxymethamphetamine (MDMA, 'Ecstasy'). *Toxicol Lett* **112–113**: 143–146.

Saxena S, Brody AL, Ho ML, Alborzian S, Maidment KM, Zohrabi N *et al* (2002). Differential cerebral metabolic changes with paroxetine treatment of obsessive–compulsive disorder *vs* major depression. *Arch Gen Psychiatry* **59**: 250–261.

Smith DF, Geday J (2001). PET neuroimaging of clomipramine challenge in humans: focus on the thalamus. *Brain Res* **892**: 193–197.

Suehiro M, Ravert HT, Dannals RF, Scheffel U, Wagner HN (1992). Synthesis of a radiotracer for studying serotonin uptake sites with positron emission tomography: [^{11}C] McN-5652-Z. *J Labelled Compd Radiopharm* **31**: 841–849.

Szabo Z, McCann UD, Wilson AA, Scheffel U, Owonikoko T, Mathews WB *et al* (2002). Comparison of (+)-[^{11}]C-McN5652 and [^{11}]C-DASB as serotonin transporter radioligands under various experimental conditions. *J Nucl Med* **43**: 678–692.

Szabo Z, Scheffel U, Mathews WB, Ravert HT, Szabo K, Kraut M *et al* (1999). Kinetic analysis of [^{11}C]McN5652: a serotonin transporter radioligand. *J Cereb Blood Flow Metab* **19**: 967–981.

Tsai SJ, Ouyang WC, Hong CJ (2002). Association for serotonin transporter gene variable number tandem repeat polymorphism and schizophrenic disorders. *Neuropsychobiology* **45**: 131–133.

Yamamoto M, Suhara T, Okubo Y, Ichimiya T, Sudo Y, Inoue M *et al* (2002). Age-related decline of serotonin transporters in living human brain of healthy males. *Life Sci* **71**: 751–757.

Zessin J, Eskola O, Brust P, Bergman J, Steinbach J, Lehikoinen P *et al* (2001). Synthesis of *S*-([^{18}F]fluoromethyl)-(+)-McN5652 as a potential PET radioligand for the serotonin transporter. *Nucl Med Biol* **28**: 857–863.

Zessin J, Gucker P, Ametamey SM, Steinbach J, Brust P, Vollenweider FX *et al* (1999). Efficient synthesis of enantiomerically pure thioester precursors of [^{11}C] McN-5652 from racemic McN-5652. *J Labelled Comp Radiopharm* **42**: 1301–1312.

Ziegler T (1991). Approximate density functional theory as a practical tool in molecular energetics and dynamics. *Chem Rev* **91**: 651–667.